Int. J. Electrochem. Sci., 14 **(2019)** 1869 – 1875, doi: 10.20964/2019.02.63

International Journal of
ELECTROCHEMICAL
SCIENCE
www.electrochemsci.org

Short Communication

Ti_4O_7 Layer Coated Sulfur Composite as High-Performance Cathode Material for Lithium-Sulfur Battery

Zhao Jinguo[*], *Liu Shoufa*

Department of Mechanical and Electrical Technology, Xijing University, Shaanxi Xi'an 710123, China
[*]E-mail: zhaojinguo@xijing.edu.cn zhaojinguoxijing@126.com

Received: 3 October 2018 / *Accepted:* 19 November 2018 / *Published:* 5 January 2019

The application of Li-S battery is hindered mainly due to the shuttle effect of the polysulfide, which is produced via discharge process. Most recently, metal oxides are applied for inhibiting this shuttle effect. In our work, mesoporous Ti_4O_7/S composites are prepared and employed into Li-S battery. The mesoporous Ti_4O_7 layer in the Ti_4O_7/S composites could provide both physical absorption and chemical bond between the polysulfide and cathode material. As a result, the electrochemical results show that the Ti_4O_7/S composites have excellent cycle stability and high specific capacity. This excellent electrochemical performance is attributed to the presence of Ti_4O_7 layer in the composite.

Keywords: Cathode; S@Ti_4O_7; Cycle stability: Capacity; Electrochemical performance

1. INTRODUCTION

During the past decades, many achievements have been obtained in the electrochemical energy storage system [1, 2]. These energy storage systems included Li-ion batteries, Li-Air batteries, Li-S batteries and so on [3, 4, 5, 6]. Among these batteries, Li-S batteries are the most promising candidate for the next generation energy storage system. This is mainly due to the high specific capacity (1675 mAh g^{-1}) and energy density (2600 Wh Kg^{-1}) of Li-S batteries [7, 8, 9]. Moreover, the sulfur has advantage of resource abundance and no pollution for the environment [10, 11]. Consequently, much attention has been paid on the research of Li-S batteries.

However, several issues hindered the application of Li-S batteries. First, the poor electronic conductivity of sulfur lead to the low discharge capacity value during discharging process [12]. Second, the soluble polysulfide will produce during the electrochemical reaction [13]. This polysulfide caused shuttle effect which had negative effect on the cycle stability. Therefore, the key factor is enhancing the

conductivity and inhibiting the shuttle effect at the same time [14] .

To address these problems, the scientists have proposed many strategies in the literature. Linda Nazar first reported the application of SBA-15 in the Li-S batteries [15]. Due to the employment of SBA-15, the as-prepared Li-S batteries showed perfect cycle stability. After that, the works about the various carbon materials become more and more, such as mesoporous carbon, carbon fiber, carbon nanotube and graphene. Until the emergence of MnO_2 in the Li-S batteries, the researchers put their eyes from the carbon to the metal oxides. The most interesting work is that Lou prepared MnO_2 nanosheet and applied it as host material for sulfur [16].

In this work, Ti_4O_7 coated sulfur composites were successfully prepared via heat treatment method. The as-prepared S@Ti_4O_7 composites exhibited excellent capacity value and cycle stability. This superior electrochemical performance is attributed to the presence of Ti_4O_7 layer in the composite. The Ti_4O_7 layer could enhance the conductivity and inhibit the shuttle effect at the same time.

2. EXPERIMENT

2.1. Preparation of S@Ti_4O_7 Composite

In this experiment, the sulfur was firstly prepared. 1.2 ml HCl was added into 120 ml $Na_2S_2O_3$ solution at the condition of stirring for 3 h. After that, the surfactant of 20 g hexadecyl trimethyl ammonium bromide (CATB) was added into the mixed solution. The next step is the growth of Ti_4O_7 layer on the sulfur particle. Typically, 20 ml titanium isopropoxide (TIP) solution was added into the above solution. Then, 2.1 ml ammonia was gradually added for the reaction with TIP forming TiO_2 layer on the surface of sulfur. After that, the sample was reduced under H_2 atmosphere for 3 h. Finally, the sample was washed and dried to obtain S@Ti_4O_7 composite.

2.2. Materials Characterization

The as-obtained samples were characterized by using a transmission electron microscope (TEM, Tecnai F20), an X-ray diffractometer (XRD, D8 Advance, BRUKER). The content of sulfur in the composite was tested by thermogravimetric analysis (TG, TA Q600 instrument).

2.3. Electrochemical Measurements

The electrochemical performance was measured by using coin-type half batteries. A slurry was prepared by mixing 80 wt.% samples, 10 wt.% super black and 10 wt.% Poly(vinylidene fluoride) PVDF with N-Methyl pyrrolidone (NMP). Then, the slurry was uniformly casted onto Al foil. The film was dried for 12 h under vacuum at 80°C and was cut into circular electrodes. The cells were assembled in an Ar-filled glove box with lithium foil, and a solution of 1.0 M bis-trifluoro methane sulfonimide lithium salt (LiTFSI) was dissolved in ethylene carbonate (EC)/ diethyl carbonate (DEC) as the electrolyte. Dicharging/charging profiles were

carried out on a battery testing system (Xin Wei) in the potential between 1.5 V and 3 V. Electrochemical impedance spectroscopy was tested on an electrochemistry workstation.

3. RESULTS AND DISSCUSIONS

To understand the morphology of the as-prepared S@Ti_4O_7 composite, SEM was conducted. As shown in Figure 1a, the S@Ti_4O_7 composite exhibits spheres structure with a dimeter of ~230 nm. To further confirm the Ti_4O_7 layer in the S@Ti_4O_7 composite, TEM was tested. As shown in Figure 1b and Figure 1c, it can be clearly seen that the S@Ti_4O_7 composite shows core-shell structure, in which the sulfur particle is coated by the Ti_4O_7 layer. Moreover, the corresponding elemental mapping (Figure d-g) of S@Ti_4O_7 composite was tested to determine the component. From the Figure e-g, it can be observed that the elements of Ti, O, S are dispersed uniformly in the whole S@Ti_4O_7 composite [17].

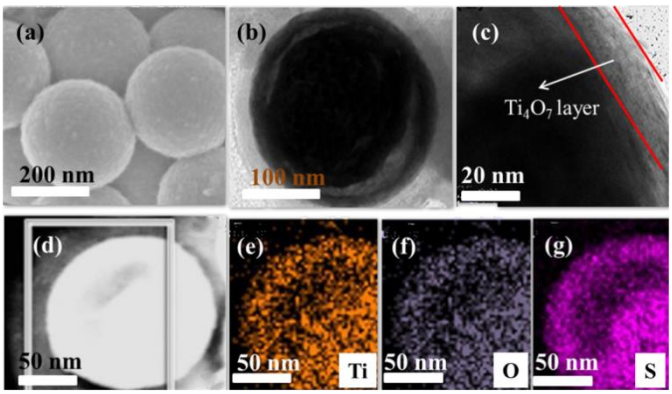

Figure 1. (a) SEM image, (b) and (c) TEM image of S@Ti_4O_7 composite, (d), (e), (f), (g) SEM image of S@Ti_4O_7 composite and corresponding elemental mapping of Ti, O, S.

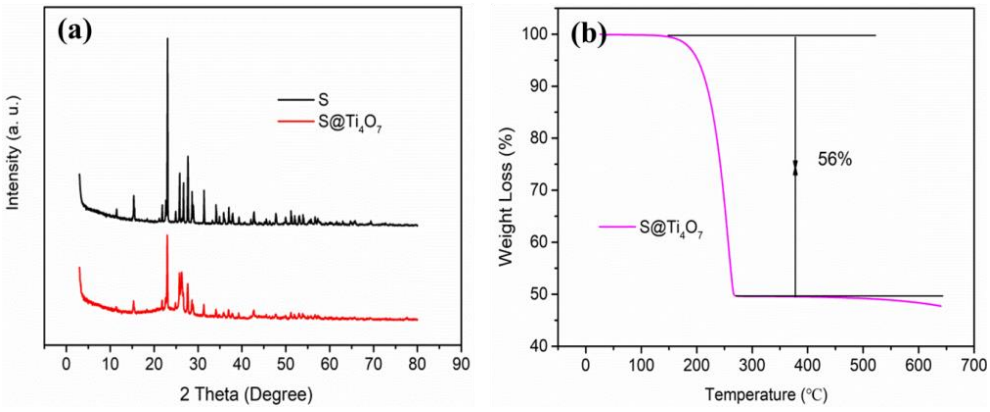

Figure 2. (a) The XRD patterns of pure sulfur and S@Ti_4O_7 composite. (b) TG curve of S@Ti_4O_7 composite.

Figure 2a is the XRD pattern of all samples. As shown in the Figure, the sulfur shows strong typical reflection pattern of S_8 molecule [18]. When the sulfur was coated by Ti_4O_7 layer, the S@Ti_4O_7 composite displays the same diffraction peak as pure sulfur. However, the peak intensity of S@Ti_4O_7

composite is weaker than the pure sulfur. This is mainly due to the presence of Ti_4O_7 layer on the surface of sulfur. Because the sulfur is covered by the Ti_4O_7 layer. Therefore, this will lead to the decrease of peak intensity. To determine the sulfur content in the S@Ti_4O_7 composite, thermogravimetric analysis was tested under Ar atmosphere. As shown in Figure 2b, the sulfur mass loss is about 56%, which demonstrates that the sulfur content in the S@Ti_4O_7 composite is 56%.

Figure 3 shows the initial discharge-charge profiles of pure sulfur and S@Ti_4O_7 composite at the current density of 0.05 C. From the figure, some information can be obtained. First, the S@Ti_4O_7 composite exhibits discharge capacity value of 1205 mAh g^{-1}, which is much higher than the pure sulfur (802 mAh g^{-1}). Second, in terms of the shape of the profiles, it can be seen that the discharge profile has two voltage platforms from 1.5 V to 3.0 V. These two voltage platforms represent two step reaction of S_8, which include the formation of soluble polysulfide and insoluble Li_2S. During the two voltage platforms, the second platform at 2.1 V provides much higher capacity value than the first platform at 2.3 V. This improved capacity value has close correlation with the presence of Ti_4O_7 layer in the S@Ti_4O_7 composite. This is because the metal oxide Ti_4O_7 could enhance the electronic conductivity of the cathode materials [19].

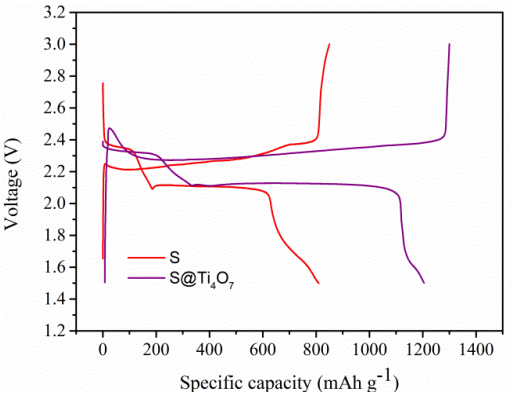

Figure 3. The initial discharge-charge profiles of pure sulfur and S@Ti_4O_7 composite.

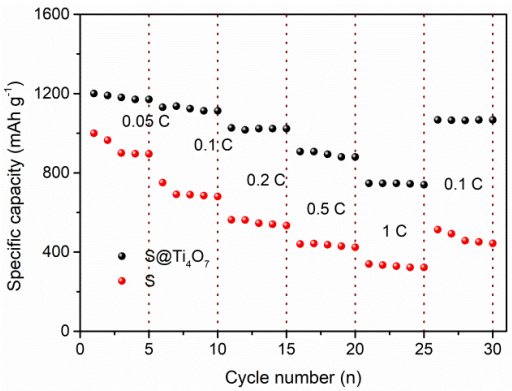

Figure 4. The rate performances of pure sulfur and S@Ti_4O_7 composite.

Rate performance is a key index for judging the electrochemical performance of the Li-S battery. Therefore, we have tested the rate performance of pure sulfur and S@Ti_4O_7 composite at various current

densities from 0.05 C to 1 C. As shown in Figure 4, the S@Ti_4O_7 composite displays capacity value of 1205 mAh g^{-1}, 1192 mAh g^{-1}, 1086 mAh g^{-1}, 1003 mAh g^{-1} at the current densities of 0.05 C, 0.1 C, 0.2 C and 0.5 C, respectively. More importantly, the discharge capacity value of S@Ti_4O_7 composite is 753 mAh g^{-1} at the current density of 1 C. However, for the pure sulfur electrode, the all capacity values of pure sulfur are lower than the S@Ti_4O_7 composite. Moreover, it can be clearly observed that the S@Ti_4O_7 composite could keep the capacity value when the current densities increase. Rate performance is related to the conductivity of the electrode materials. Therefore, the S@Ti_4O_7 composite shows more excellent rate performance than the pure sulfur electrode [20, 21].

The cycle performances of pure sulfur and S@Ti_4O_7 composite are shown in Figure 5a. As it can be seen from the Figure, the S@Ti_4O_7 composite demonstrates superior cycle stability than the pure sulfur. The capacity value of S@Ti_4O_7 composite remains 708 mAh g^{-1} after 100 cycles. While the capacity value of pure sulfur is only 483 mAh g^{-1} after 100 cycles. Although the capacity fade rapidly at first 20 cycles for S@Ti_4O_7 composite, however, after that, the capacity value becomes stable. In a word, the S@Ti_4O_7 composite shows more excellent cycle stability than the pure sulfur.

Electrochemical impedance spectroscopy was measured on an electrochemistry workstation. As shown in Figure 5b, the as-prepared S@Ti_4O_7 composite has a smaller diameter of the high frequency semicircle, demonstrating much lower interface layer resistance than pure sulfur. This result further confirms that the S@Ti_4O_7 composite exhibits more superior conductivity than the pure sulfur electrode. As a result, the electronics could easily transport in the channels of the cathode materials. Besides, it is beneficial for the Li^+ transfer in the electrolyte between electrode surface and electrolyte [22, 23].

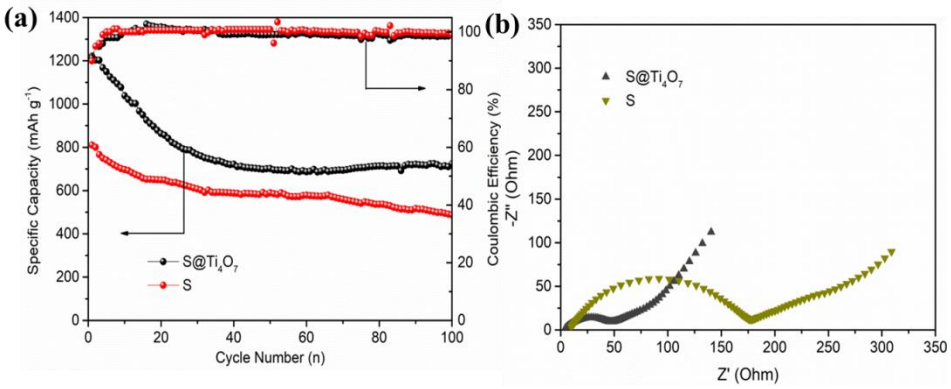

Figure 5. (a) The cycle performances of pure sulfur and S@Ti_4O_7 composite. (b) The electrochemical impedance spectra of pure sulfur and S@Ti_4O_7 composite.

Table 1 lists the electrochemical performance of similar cathode materials for Li-S battery. As shown in Table 1, it can be clearly seen that the S@Ti_4O_7 composite displays superior cycle stability

among these similar cathode materials. This indicates that the S@Ti_4O_7 composite would be a promising cathode material for the Li-S battery.

Table1. The comparison between S@Ti_4O_7 composite and other similar cathode materials

Samples	Current Density	Capacity	Reference
S@MnO_2@GO	0.2 C	405 (100)	24
S/C-SnS_2	0.2 C	698 (100)	25
PEDOT/TiO_2/S	0.1 C	532 (100)	26
S@Ti_4O_7	0.2 C	708 (100)	This Work

4. CONCLUSIONS

a) The yolk-shell structure S@Ti_4O_7 composite was successfully prepared and used as cathode materials for Li-S batteries.

b) The S@Ti_4O_7 composite showed high capacity value and excellent cycle stability.

c) The superior electrochemical performances are attributed to the yolk-shell structure, which could protect the polysulfide in the cathode side. Moreover, the metal oxide Ti_4O_7 layer could improve the electronic conductivity.

ACKNOWLEDGMENTS
This research is financially supported by Research Project of Shaanxi Provincial Education Departmen t (15JK2186).

References

1. J. Liu, M. F. Wang, N. Xu, T. Qian and C. L. Yan, *Energ. Storage Mater*., 15 (2018) 53.
2. Y. L. An, Y. Tian, H. F. Fei, G. F. Zeng, H. W. Duan, S. C. Zhang, P. Zhou, L. J. Ci and J. K. Feng, *Mater. Lett*., 228 (2018) 175.
3. Y. Li, J. Chen, Y. F. Zhang, Z. Y. Yu, T. Z. Zhang, W. Q. Ge and L. P. Zhang, *J. Alloy Compd*., 766 (2018) 804.
4. H. J. Zhao, N. P. Deng, J. Yan, W. M. Kang, J. G. Ju,Y. L. Ruan, X. Q. Wang, X. P. Zhuang, Q. X. Li and B. W. Chen, *Chem. Eng. J*., 347 (2018) 343.
5. P. H. Ji, B. Shang, Q. M. Peng, X. B. Hu and J. W. Wei, *J. Power Sources*, 400 (2018) 572.
6. W. T. Tsou, C. Y. Wu, H. Yang and J. G. Duh, *Electrochim. Acta*, 285 (2018) 16.
7. Y. Q. Wang, S. Q. Luo, D. Q. Wang, X. B. Hong and S. K. Liu, *Electrochim. Acta*, 284 (2018) 400.
8. Y. Z. Song, W. Zhao, N. Wei, L. Zhang, F. Ding, Z. F. Liu and J. Y. Sun, *Nano Energ*., 53 (2018) 432.
9. N. Liu, L. Wang, Y. Zhao, T. Z. Tan and Y. G. Zhang, *J. Alloy Compd*., 769 (2018) 678.
10. Q. Cheng, C. Liu, K. Meng, X. H. Yu, Y. N. Zhang, J. X. Liu, X. Jin and L. Y. Jin, *Int. J. Electrochem. Sci*., 13 (2018) 265.
11. J. Q. Guo, J. Li, Y. J. Huang, M. Zeng and R. F. Peng, *Mater. Lett*., 181 (2016) 289.
12. X. B. Liu, X. F. Shao, F. Li and M. W. Zhao, *Appl. Surf. Sci*., 455 (2018) 522.

13. Z. W. Ding, D. L. Zhao, R. R. Yao, C. Li, X. W. Cheng, T. Hu, *Int. J. Hydrogen Energ*., 43 (2018) 10502.
14. H. F. Shi, S. Z. Niu, W. Lv and Q. H. Yang, *Carbon*, 138 (2018) 18.
15. X. L. Ji, S. Evers, R. Black and L. F. Nazar, *Nat. Commun*., 2 (2011) 325.
16. Z. Li, J. T. Zhang and X. W. Lou, *Angew. Chem. Int. Edit*., 54 (2015) 12886.
17. L. S. Fan, H. X. Wu, X. Wu, M. X. Wang, J. H. Cheng, N. Q. Zhang, Y. J. Feng and K. N. Sun, *Electrochim. Acta*, 19 (2018) 137.
18. S. Li, Z. G. Luo, X. X. Cao, G. Z. Fang and S. Q. Liang, *Int. J. Electrochem. Sci*., 13 (2018) 23.
19. X. Song, T. Gao, S. Q. Wang, Y. Bao, G. P. Chen, L. X. Ding and H. H. Wang, *J. Power Sources*, 356 (2017) 172.
20. Y. Gong, C. P. Fu, G. P. Zhang, H. H. Zhou and Y. F. Kuang, *Electrochim. Acta*, 256 (2017) 1.
21. C. Zheng, S. Z. Niu, W. Lv, G. M. Zhou, J. Li, S. X. Fan, Y. Q. Deng, Z. Z. Pan, B. H. Li, F. Y. Kang and Q. H. Yang, *Nano Energ*., 33 (2017) 306.
22. L. L. Yan, M. Xiao, S. J. Wang, D. M. Han and Y. Z. Meng, *J. Energ. Chem*., 26 (2017) 522.
23. X. Y. Qian, D. Zhao, L. N. Jin, X. Q. Shen, S. S. Yao, D. W. Rao, Y. Y. Zhou and X. M. Xi, *Mater. Res. Bull*., 94 (2017) 104.
24. X. K. Huang, K. Y. Shi, J. Yang, G. Mao and J. H. Chen, *J. Power Sources*, 356 (2017) 72.
25. M. Li, J. B. Zhou, J. Zhou, C. Guo, Y. Han, Y. C. Zhu, G. M. Wang and Y. T. Qian, *Mater. Res. Bull*., 96 (2017) 509.
26. K. J. Luan, S. S. Yao, Y. J. Zhang, R. Y. Zhuang, J. Xiang, X. Q. Shen, T. B. Li, K. S. Xiao and S. B. Qin, *Electrochim. Acta*, 252 (2017) 461.